Layered Iron(III) Arsenates: Synthesis and Characterization of $A_2Fe_2O(AsO_4)_2$ (A = K, Rb)

Rei-Shyang Chang,† Sue-Lein Wang,† and Kwang-Hwa Lii*,‡

Department of Chemistry, National Tsing Hua University, Hsinchu, and Institute of Chemistry, Academia Sinica, Taipei, Taiwan, ROC

Received January 2, 1997[⊗]

Two new iron(III) arsenates $K_2Fe_2O(AsO_4)_2$ (**1**) and $Rb_2Fe_2O(AsO_4)_2$ (**2**) have been synthesized and characterized by single-crystal X-ray diffraction, magnetic susceptibilities, and Mossbauer spectroscopy. The two compounds are isostructural and exhibit a sheet structure consisting of infinite slabs of edge-sharing FeO_6 octahedra linked into sheets by AsO_4 tetrahedra, with the alkali-metal cations in the interlayer region. Crystal data for **1**: orthorhombic, space group *Pnma* (No. 62), $a = 8.5219(3)$ Å, $b = 5.7612(2)$ Å, $c = 17.9452(6)$ Å, $Z = 4$. Crystal data for **2**: As above, except $a = 8.5330(2)$ Å, $b = 5.7945(2)$ Å, $c = 18.6157(1)$ Å. Room-temperature Mossbauer data confirm the presence of Fe^{III}. Magnetic susceptibility measurements on compound **2** show that it undergoes a transition to a weak ferromagnetic state near 25 K.

Introduction

Iron phosphates are of interest by virtue of applications to corrosion inhibition and catalysis, as well as for their rich structural chemistry and interesting magnetic properties.[1] The synthesis of iron phosphates calls upon several methods: hydrothermal, flux, and high-temperature solid-state reactions. We have recently described the hydrothermal syntheses and crystal structures of a number of new ternary iron phosphates.[2] These compounds present a variety of complex crystal structures and are a challenge to complete characterization. Their structures cover discrete FeO_6 octahedra, FeO_5 trigonal bipyramids, dimers of corner-sharing, edge-sharing, or face-sharing FeO_6 octahedra, trimeric and tetrameric units of Fe−O polyhedra, and infinite chains of FeO_6 octahedra sharing either trans or skew edges. They include iron(II), iron(III), and mixed-valence compounds. Compared to iron phosphates, little work has been carried out on the arsenates. Recently, we reported the hydrothermal synthesis of a novel iron(III) arsenate, $Cs_3Fe_5O(OH)(AsO_4)_5$, whose framework structure consists of four-, five-, and six-coordinated iron atoms.[3] D'Yvoire et al. reported $Na_3Fe_2(AsO_4)_3$ which exhibits two polymorphs: a low-temperature, garnet-type form and a high-temperature, rhombohedral form.[4] The framework of the high-temperature form consists of a tetramer of edge-sharing FeO_6 octahedra. In an attempt to prepare the potassium and rubidium analogues of $Na_3Fe_2(AsO_4)_3$ by a flux method, two iron(III) arsenates with a new structure type were isolated. Herein we report the synthesis, single-crystal X-ray structures, Mossbauer spectroscopy, and magnetic susceptibilities of $K_2Fe_2O(AsO_4)_2$ and $Rb_2Fe_2O(AsO_4)_2$, the first iron arsenates to possess a sheet structure.

* To whom correspondence should be addressed.
† National Tsing Hua University.
‡ Academia Sinica.
⊗ Abstract published in *Advance ACS Abstracts,* July 1, 1997.

(1) Gleitzer, C. *Eur. J. Solid State Inorg. Chem.* **1991**, *28*, 77 and references cited therein.
(2) Lii, K.-H.; Dong, T.-Y.; Cheng, C.-Y.; Wang, S.-L. *J. Chem. Soc., Dalton Trans*. **1993**, 577. Lii, K.-H.; Shih, P.-F.; Chen, T.-M. *Inorg. Chem*. **1993**, *32*, 4373. Dvoncova, E.; Lii, K.-H. *Inorg. Chem.* **1993**, *32*, 4368. Lii, K.-H. *J. Chem. Soc., Dalton Trans*. **1994**, 931. Lii, K.-H.; Huang, C.-Y. *J. Chem. Soc., Dalton Trans*. **1995**, 571; *Eur. J. Solid State Inorg. Chem.* **1995**, *32*, 225. Lii, K.-H. *Eur. J. Solid State Inorg. Chem*. **1995**, *32*, 225; *J. Chem. Soc., Dalton Trans*. **1996**, 819.
(3) Wang, B.; Wang, S.-L.; Lii, K.-H. *J. Chem. Soc., Chem. Commun.* **1996**, 1061.
(4) D'Yvoire, F.; Pintard-Screpel, M.; Bretey, E. *Solid State Ionics* **1986**, *18*−19, 502.

Experimental Section

Synthesis. RbH_2AsO_4 was prepared from a solution of As_2O_3 dissolved in H_2O_2 with rubidium hydroxide. KH_2AsO_4 was from Sigma Chemical Co. In an attempt to prepare the potassium and rubidium analogs of $Na_3Fe_2(AsO_4)_3$ a mixture of 1 mmol of KH_2AsO_4 (or RbH_2AsO_4) and 0.333 mmol of Fe_2O_3 was placed in a 15-mL platinum crucible and thermally treated as follows: heat from RT (room temperature) to 800 °C over 8 h; maintain at 800 °C for 1 h; cool to 600 °C at 5 °C/h; quench to RT by removing the crucible from the furnace. Excess alkali-metal dihydrogen arsenates served as fluxes for crystal growth. The products were washed with hot water to remove the fluxes, and the solid products were obtained by suction filtration. The products contained red crystals of the title compounds. On the basis of X-ray analysis using a Siemens powder diffractometer, monophasic $Rb_2Fe_2O(AsO_4)_2$ was prepared by reaction of RbH_2AsO_4 and Fe_2O_3 in a mole ratio of 2:1 at 700 °C for 2 d with several intermediate grindings. The sample was used for Mossbauer spectroscopy and magnetic susceptibility measurements (vide infra). In the case of $K_2Fe_2O(AsO_4)_2$, the product was always contaminated with a small amount of unidentified yellow material. In a reaction to synthesize the cesium analog of the title compounds under similar reaction conditions, we have isolated and structurally characterized $Cs_7Fe_7O_2(AsO_4)_8$ which is isostructural with the corresponding phosphate $Cs_7Fe_7O_2(PO_4)_8$.[5]

Single-Crystal X-ray Diffraction. Two red crystals of dimensions 0.65 × 0.28 × 0.20 mm for $K_2Fe_2O(AsO_4)_2$ (**1**) and 0.14 × 0.12 × 0.05 mm for $Rb_2Fe_2O(AsO_4)_2$ (**2**) were selected for indexing and intensity data collection on a Siemens Smart-CCD diffractometer equipped with a normal focus, 3 kW sealed-tube X-ray source. Intensity data were collected in 1200 frames with increasing ω (width of 0.3° per frame). Unit cell dimensions were determined by a least-squares fit of 3495 and 2577 reflections for compounds **1** and **2**, respectively. 2θ range: 3−53° for both compounds. Number of measured reflections and observed unique reflections ($I > 2.5\,\sigma(I)$): 4153, 915 for **1**; 4425, 837 for **2**. Agreement between equivalent reflections (R_{int}): 0.041 for **1** and 0.035 for **2**. Absorption corrections for **1** and **2** were based on 3595 and 3032 symmetry-equivalent reflections, respectively, using the SHELXTL PC program package ($T_{min,\ max}$: 0.330, 0.886 for **1**; 0.320, 0.973 for **2**).[6] On the basis of systematic absences, statistics of intensity distribution, and successful solution and refinement of the structures, the space group for both compounds was determined to be *Pnma* (No. 62). The structure was solved by direct methods: The metal and arsenic atoms were first located and all the oxygen atoms were found in

(5) Andrews-Allen, E. M.; Robinson, W. R. *J. Solid State Chem.* **1988**, *74*, 88.
(6) Sheldrick, G. M. *SHELXTL PC, Version 5*; Siemens Analytical X-Ray Instruments, Inc.: Madison, WI, 1995.

S0020-1669(97)00004-9 CCC: $14.00

Table 1. Crystallographic Data for $K_2Fe_2O(AsO_4)_2$ (**1**) and $Rb_2Fe_2O(AsO_4)_2$ (**2**)

	1	**2**
chem formula	$As_2Fe_2K_2O_9$	$As_2Fe_2O_9Rb_2$
fw	483.74	576.48
space group	*Pnma* (No. 62)	*Pnma* (No. 62)
a, Å	8.5219(3)	8.5330(2)
b, Å	5.7616(2)	5.7945(2)
c, Å	17.9452(6)	18.6157(1)
V, Å^3	881.1(1)	920.4(1)
Z	4	4
μ(Mo Kα), cm^{-1}	117.2	208.2
ρ_{calcd}, g·cm^{-3}	3.647	4.160
λ, Å	0.710 73	0.710 73
T, °C	23	23
R^a	0.0351	0.0299
$R_w{}^b$	0.0435	0.0356

[a] $R = \sum||F_o| - |F_c||/\sum|F_o|$. [b] $R_w = [\sum w(|F_o| - |F_c|)^2/\sum w|F_o|^2]^{1/2}$, $w^{-1} = \sigma^2(F) + gF^2$, where $g = 0.00181$ and 0.00235 for **1** and **2**, respectively.

Table 2. Atomic Coordinates and Thermal Parameters (Å^2 × 100) for $K_2Fe_2O(AsO_4)_2$ (**1**) and $Rb_2Fe_2O(AsO_4)_2$ (**2**)

atom	*x*	*y*	*z*	$U_{eq}{}^a$
		Compound **1**		
K(1)	−0.0432(2)	0.75	0.2662(1)	0.0299(6)
K(2)	0.6001(2)	0.25	0.36697(9)	0.0192(5)
Fe(1)	−0.2853(1)	0.25	0.56688(5)	0.0072(3)
Fe(2)	0	0	0.5	0.0064(3)
As(1)	0.32439(7)	0.25	0.55910(4)	0.0062(3)
As(2)	0.18272(7)	0.25	0.35236(4)	0.0073(3)
O(1)	0.5072(5)	0.25	0.5244(3)	0.013(1)
O(2)	0.3197(5)	0.25	0.6507(3)	0.018(2)
O(3)	0.2333(4)	0.0090(5)	0.5242(2)	0.0099(9)
O(4)	0.0866(6)	0.25	0.2735(3)	0.024(2)
O(5)	0.0444(5)	0.25	0.4225(2)	0.006(1)
O(6)	0.3006(4)	0.0126(5)	0.3618(2)	0.0117(9)
O(7)	−0.0585(5)	0.25	0.5653(2)	0.005(1)
		Compound **2**		
Rb(1)	−0.0380(1)	0.75	0.26778(6)	0.0288(4)
Rb(2)[b]	0.6106(4)	0.25	0.36303(6)	0.0208(4)
Rb(2′)[b]	0.702(4)	0.25	0.352(1)	0.0208(4)
Fe(1)	−0.2842(1)	0.25	0.56544(7)	0.0097(4)
Fe(2)	0	0	0.5	0.0088(4)
As(1)	0.3241(1)	0.25	0.55595(5)	0.0087(3)
As(2)	0.1795(1)	0.25	0.35720(5)	0.0104(3)
O(1)	0.5090(7)	0.25	0.5256(4)	0.018(2)
O(2)	0.3174(8)	0.25	0.6448(3)	0.018(2)
O(3)	0.2326(5)	0.0105(6)	0.5219(2)	0.013(1)
O(4)	0.0846(9)	0.25	0.2808(4)	0.024(2)
O(5)	0.0396(7)	0.25	0.4234(3)	0.010(2)
O(6)	0.2960(5)	0.0128(7)	0.3657(2)	0.014(1)
O(7)	−0.0574(7)	0.25	0.5634(3)	0.008(2)

[a] U_{eq} is defined as one-third of the trace of the orthogonalized $\mathbf{U}_{ij}$ tensor. [b] The occupancy factors of Rb(2) and Rb(2′) are 0.948(2) and 0.052(2), respectively.

difference Fourier maps. For $Rb_2Fe_2O(AsO_4)_2$, atom Rb(2) exhibited a large U_{11} value and a large residual electron density (4.0 e/Å^3) at a distance of 0.95 Å from Rb(2), which could be interpreted as disorder between two sites. Therefore, a model of two disordered sites for Rb(2) was used with constraints applied to their occupancy factors and thermal parameters. The thermal parameters for two disordered Rb(2) sites were constrained to be the same, and the sum of their occupancy factors was set equal to 1. The refinement results were 94.8(2) and 5.2(2)% occupancies for Rb(2) and Rb(2′). In contrast, the potassium atoms in **1** did not reveal any disorder. The final cycles of least-squares refinement including the atomic coordinates and anisotropic thermal parameters for all atoms converged at $R = 0.035$ for **1** and $R = 0.030$ for **2**. Neutral-atom scattering factors for all atoms were used. Anomalous dispersion and secondary extinction corrections were applied. Structure solution and refinement were performed by using SHELXTL PC programs.

Table 3. Bond Lengths (Å) and Valence Sums (∑s) for $K_2Fe_2O(AsO_4)_2$ (**1**) and $Rb_2Fe_2O(AsO_4)_2$ (**2**)

	Compound **1**		
Fe(1)−O(1)	1.925(4)	Fe(1)−O(3)	2.257(3) (2×)
Fe(1)−O(6)	1.986(3) (2×)	Fe(1)−O(7)	1.933(4)
	∑s(Fe(1)−O) = 2.68		
Fe(2)−O(3)	2.036(3) (2×)	Fe(2)−O(5)	2.038(3) (2×)
Fe(2)−O(7)	1.923(3) (2×)		
	∑s(Fe(2)−O) = 2.96		
As(1)−O(1)	1.677(4)	As(1)−O(2)	1.644(5)
As(1)−O(3)	1.710(3) (2×)		
	∑s(As(1)−O) = 5.00		
As(2)−O(4)	1.635(5)	As(2)−O(5)	1.724(4)
As(2)−O(6)	1.706(3) (2×)		
	∑s(As(2)−O) = 4.91		
K(1)−O(2a)	2.789(5)	K(1)−O(2b)	2.816(5)
K(1)−O(4)	3.089(2) (2×)	K(1)−O(6)	3.057(4) (2×)
K(1)−O(7)	3.144(5)		
	∑s(K(1)−O) = 0.71		
K(2)−O(1)	2.935(5)	K(2)−O(2)	2.978(1) (2×)
K(2)−O(3)	2.838(3) (2×)	K(2)−O(4)	2.523(5)
K(2)−O(6)	2.897(3) (2×)		
	∑s(K(2)−O) = 1.21		
	Compound **2**		
Fe(1)−O(1)	1.914(7)	Fe(1)−O(3)	2.262(4) (2×)
Fe(1)−O(6)	1.993(4) (2×)	Fe(1)−O(7)	1.936(6)
	∑s(Fe(1)−O) = 2.67		
Fe(2)−O(3)	2.027(4) (2×)	Fe(2)−O(5)	2.061(4) (2×)
Fe(2)−O(7)	1.932(4) (2×)		
	∑s(Fe(2)−O) = 2.90		
As(1)−O(1)	1.675(7)	As(1)−O(2)	1.654(6)
As(1)−O(3)	1.714(4) (2×)		
	∑s(As(1)−O) = 4.95		
As(2)−O(4)	1.637(7)	As(2)−O(5)	1.715(6)
As(2)−O(6)	1.704(4) (2×)		
	∑s(As(2)−O) = 4.94		
Rb(1)−O(2a)	2.887(7)	Rb(1)−O(2b)	2.964(7)
Rb(1)−O(4)	3.090(4) (2×)	Rb(1)−O(6)	3.241(4) (2×)
Rb(1)−O(7)	3.247(6)		
	∑s(Rb(1)−O) = 0.76		
Rb(2)−O(1)	3.149(7)	Rb(2)−O(2)	2.965(2) (2×)
Rb(2)−O(3)	2.943(4) (2×)	Rb(2)−O(4)	2.686(7)
Rb(2)−O(6)	3.016(4) (2×)		
	∑s(Rb(2)−O) = 1.29		
Rb(2′)−O(2)	2.903(2) (2×)	Rb(2′)−O(3)	2.85(2) (2×)
Rb(2′)−O(4)	2.67(2)	Rb(2′)−O(5)	3.17(3)
	∑s(Rb(2′)−O) = 1.19		

Mossbauer Spectroscopy and Magnetic Susceptibility. The ^{57}Fe Mossbauer measurements were made on a constant-acceleration instrument at room temperature. A 99.99% pure 10 μm iron foil was employed as the standard. Isomer shifts are reported with respect to the standard at 300 K. Variable-temperature magnetic susceptibility $\chi(T)$ data were obtained on 46.9 mg of polycrystalline sample from 2 to 300 K in a magnetic field of 3 kG after zero-field cooling using a SQUID magnetometer. Susceptibility measurements were also performed at 16 K in several different applied fields between 1 and 10 kG. The sample showed field dependence of χ at 16 K. Correction for diamagnetism was made according to Selwood.[7]

Results and Discussion

Crystal Structures. The crystallographic data are listed in Table 1. The atomic coordinates, bond lengths, and bond-valence sums[8] are given in Tables 2 and 3, respectively. Atom Fe(2) is located at inversion centers, and all other metal and arsenic and most oxygen atoms are on mirror planes. The Fe

(7) Selwood, P. W. *Magnetochemistry*; Interscience: New York, 1956.
(8) Brown, I. D.; Altermatt, D. *Acta Crystallogr.* **1985**, *B41*, 244.

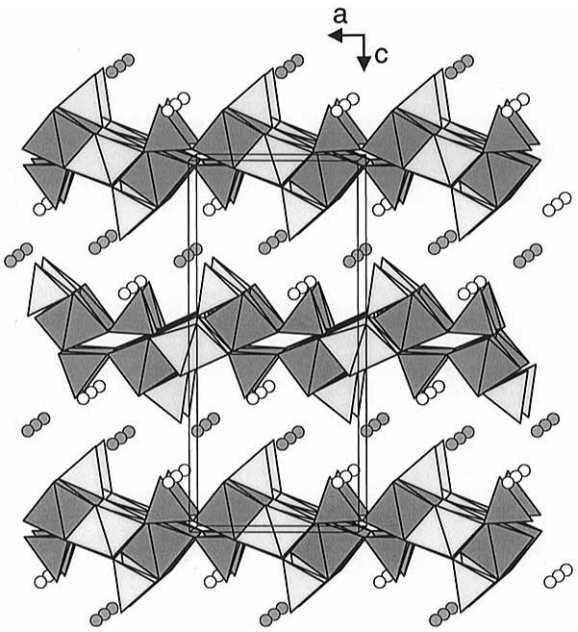

Figure 1. Polyhedral representation of the $Rb_2Fe_2O(AsO_4)_2$ structure viewed in a direction approximately parallel to the *b*-axis: Octahedra with darker shading, $Fe(1)O_6$; octahedra with lighter shading, $Fe(2)O_6$; tetrahedra with darker shading, $As(1)O_4$; tetrahedra with lighter shading, $As(2)O_4$; circles with shading, Rb(1); open circles, Rb(2). The minor Rb(2′) site is not shown for clarity.

and As atoms are six- and four-coordinated, respectively. In the following, only the structure of $Rb_2Fe_2O(AsO_4)_2$ will be discussed in detail because the two compounds are isostructural.

The structure of $Rb_2Fe_2O(AsO_4)_2$ consists of iron−arsenate layers in the *ab*-plane with the interlayer space filled with rubidium cations, as illustrated in the perspective view parallel to the [010] direction (Figure 1). There are two iron−arsenate layers within the repeat distance *c*. The interlayer distance is decreased from 9.31 to 8.97 Å when the rubidium cations are replaced by the smaller potassium cations. Adjacent layers are symmetry related by *a*-glide planes perpendicular to the *c*-axis at $z = {}^1/_4$ and ${}^3/_4$. Within a layer there are slabs of edge-sharing FeO_6 octahedra running along the *b*-axis. Each slab contains two close packed layers of oxygen atoms with ${}^2/_3$ of the octahedral holes being occupied by Fe atoms. Adjacent slabs are connected by arsenate groups via corner sharing (Figure 2).

The building units of $Rb_2Fe_2O(AsO_4)_2$ and atom-labeling scheme are shown in Figure 3. Each $Fe(1)O_6$ octahedron shares two cis edges with two $Fe(2)O_6$ octahedra. Each $Fe(2)O_6$ octahedron shares four edges with two $Fe(1)O_6$ and two $Fe(2)O_6$ octahedra. There are numerous ways of selecting four edges from the twelve available from an octahedron. The choice of four edges in $Fe(2)O_6$ is the same as that found in crystalline Nb_3I_8.[9] Both the $Fe(1)O_6$ and $Fe(2)O_6$ octahedra, as indicated from the O···O distances, are strongly distorted. The $Fe(2)O_6$ octahedron is more regular than $Fe(1)O_6$, as observed from a comparison with Fe−O bond lengths. Atom Fe(1) is displaced from the centroid of its Fe−O octahedron away from two neighboring Fe(2) atoms by 0.283 Å, whereas Fe(2) is at the centroid of its octahedron. The valence sum for Fe(2) is in good agreement with its formal oxidation state. The lower value for Fe(1) can be correlated with the much longer Fe(1)−O(3) bond lengths as a result from the strong distortion. To better shield the positive charges on iron metal cations, the shared edges are considerably shorter than all the other edges which are not chared. The arsenate groups coordinate to iron atoms

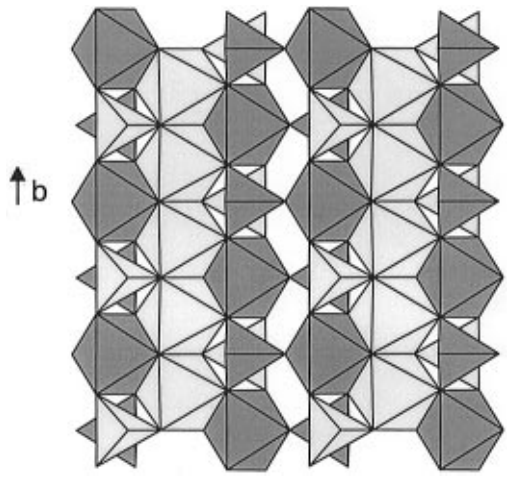

Figure 2. Layer of the $Rb_2Fe_2O(AsO_4)_2$ structure viewed along the [$\bar{1}$01] direction: Octahedra with darker shading, $Fe(1)O_6$; octahedra with lighter shading, $Fe(2)O_6$; tetrahedra with darker shading, $As(1)O_4$; tetrahedra with lighter shading, $As(2)O_4$.

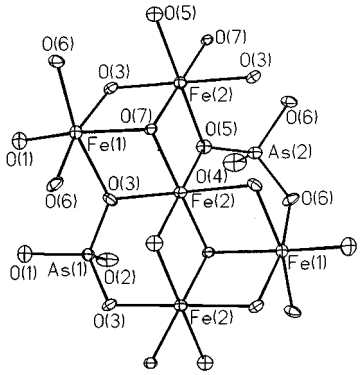

Figure 3. View of a fragment of the $Rb_2Fe_2O(AsO_4)_2$ structure showing the atom-labeling scheme (60% thermal ellipsoilds).

through three oxygen donors; the fourth oxygen is present as a pendant As=O unit and protrudes into the interlayer region. Two of the oxygen donors of $As(1)O_4$ bond to adjacent Fe(1) and Fe(2) within a slab as bridging ligands while the third oxygen coordinates to Fe(1) belonging to an adjacent slab. $As(2)O_4$ coordinates to four iron atoms within the same slab. One of the $As(2)O_4$ oxygens serves as a bridging ligand between two Fe(2) atoms. The AsO_4 tetrahedra are distorted, as indicated from the As−O bond lengths. The shortest As−O bond in each tetrahedron involves the oxygen atom which projects into the interlayer space and coordinates to alkali-metal cations only.

The coordination number of each Rb cation was determined on the basis of the maximum gap in the Rb−O distances. The maximum cation−anion distance, L_{max}, according to Donnay and Allmann was also considered (L_{max} = 3.42 Å for Rb−O and 3.35 Å for K−O).[10] Therefore, Rb(1) and Rb(2) are coordinated by seven and eight oxygen atoms with the eighth Rb(1)−O and the ninth Rb(2)−O distances at 3.71 and 3.70 Å, respectively. The coordination polyhedron of Rb(1) approximates a strongly distorted octahedron with one of the triangular faces being capped by an oxygen atom. The valence sum for Rb(1) is significantly smaller than 1, indicating that it is loosely bound. The coordination sphere of Rb(2) is highly asymmetrical and has an open space along the [100] direction, as shown in Figure 4. Consequently, Rb(2) is disordered over two sites along [100] and has a large U_{11} value. The Rb(2′) site is surrounded by six oxygen atoms. The coordination polyhedra

(9) Simon, A.; Schnering, H. G. von *J. Less-Common Met.* **1966**, *11*, 31.

(10) Donnay, G.; Allmann, R. *Am. Mineral.* **1970**, *55*, 1003.

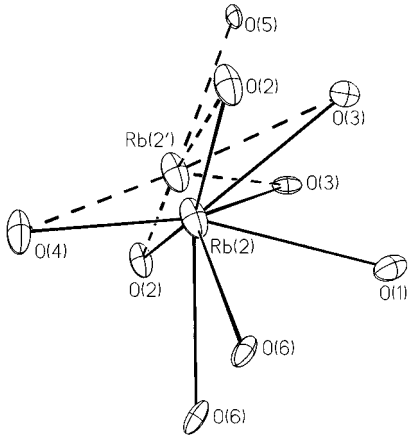

Figure 4. Coordination environment of the major Rb(2) site and the minor Rb(2′) site in $Rb_2Fe_2O(AsO_4)_2$.

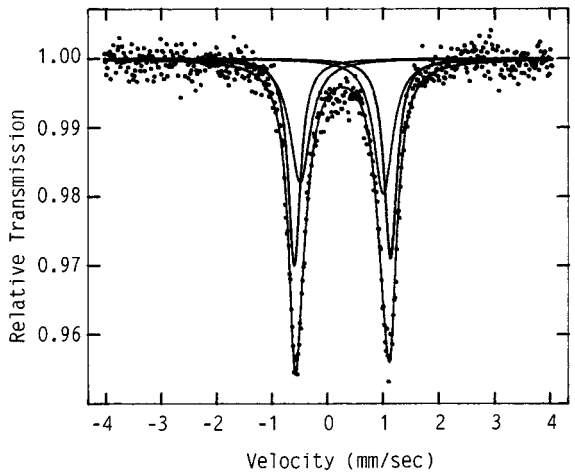

Figure 5. Mossbauer spectrum of $Rb_2Fe_2O(AsO_4)_2$ at 300 K.

of the K atoms in **1** are similar to those of the Rb atoms in **2**. The reason that K(2) is not disordered is unclear to us.

Mossbauer Spectroscopy and Magnetic Measurements. As shown in Figure 5, the room-temperature Mossbauer spectrum of $Rb_2Fe_2O(AsO_4)_2$ was least-squares fitted with two doublets with a constraint on the area ratio of 1:1. The obtained parameters are δ (isomer shift) = 0.36, 0.37 mm/s, ΔE_Q (quadrupole splitting) = 1.49, 1.72 mm/s, and Γ (full width at half-height) = 0.40, 0.44; 0.27, 0.26 mm/s. The isomer shifts for both components are characteristic of high-spin Fe(III). According to Menil, the usual ranges of isomer shifts in oxides are 0.29−0.50 and 1.03−1.28 mm/s for Fe(III) and Fe(II) in 6-coordination, respectively.[11] The component with large quadrupole splitting can be assigned to Fe(1) because it has a larger octahedral distortion.

The slabs of edge-sharing FeO_6 octahedra within the layers of the structure give rise to interesting magnetic behavior from the interactions between neighboring Fe(III) centers. Figure 6 displays the plots of molar susceptibility (χ_M) and inverse molar susceptibility ($1/\chi_M$) versus temperature for $Rb_2Fe_2O(AsO_4)_2$. The $\chi_M T$ value decreases with decreasing temperature, indicating the main magnetic interactions between Fe atoms are antiferromagnetic. In particular, the effective magnetic moment at 300 K is only 3.98 μ_B/Fe as compared with 5.92 μ_B/Fe theoretically expected for spin-only and noninteracting Fe^{3+} ions.

(11) Menil, F. *J. Phys. Chem. Solids* **1985**, *46*, 763.

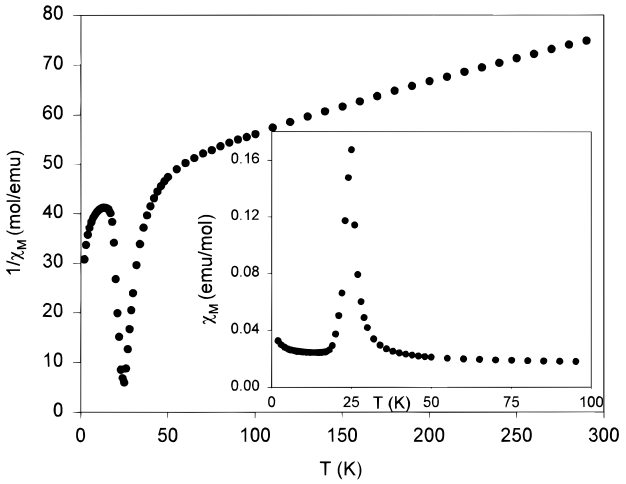

Figure 6. Molar susceptibity (χ_M) and inverse molar susceptibity ($1/\chi_M$) plotted as a function of tempterature for a powder sample of $Rb_2Fe_2O(AsO_4)_2$.

The antiferromagnetic interactions are large so that χ_M is considerably reduced from expected noninteracting moment even at room temperature. At about 25 K, the compound undergoes a transition to long-range three-dimensional order as suggested by the sharp increase in χ_M upon cooling and the observation of field-dependent χ_M below the critical temperature. The apparent ferromagnetic rise in χ_M can be interpreted as canted antiferromagnetism or alternatively so-called weak ferromagnetism. At lower temperatures the magnetic moments of the two spin lattices reach equivalency and the net moment diminishes. This is possible because the unequal moments on the two sublattices are due to symmetry-related magnetic effects and not a different number of electron on each site. Below about 13 K, there is an increase in χ_M (or decrease in χ_M^{-1}), which is likely due to the presence of magnetic impurities. The magnetic behavior of $Rb_2Fe_2O(AsO_4)_2$ is similar to that of $Fe_2(SO_4)_3$.[12]

Few synthetic iron arsenates have been reported although a good number iron arsenate minerals exist. It is interesting to note that all iron arsenates except $Na_7Fe_4(AsO_4)_6$[13] were found to contain iron in the trivalent state only. The title compounds, $K_2Fe_2O(AsO_4)_2$ and $Rb_2Fe_2O(AsO_4)_2$, are not only the first examples in the systems K/Fe/As/O and Rb/Fe/As/O but also the first iron arsenates to possess a sheet structure. The fact that a large number of iron phosphates have been synthesized suggests that there should likewise be numerous synthetic FeAsO frameworks accessible.

Acknowledgment. We thank the Institute of Chemistry, Acedemia Sinica, and the National Science Council (Grant NSC86-2113-M-001-014 to K.-H.L.; Grant NSC86-2113-M-007-011 to S.-L.W.) for support and Professor T.-Y. Dong at National Sun Yat-Sen University for Mossbauer spectroscopy measurements.

Supporting Information Available: Tables giving crystal data and details of the structure determination, anisotropic thermal parameters, interatomic distances, and bond angles (5 pages). Ordering information is given on any current masthead page.

IC970004D

(12) Long, G. J.; Longworth, G.; Battle, P.; Cheetham, A. K.; Thundathil, R. V.; Beveridge, D. *Inorg. Chem.* **1979**, *18*, 624.
(13) Masquelier, C.; d'Yvoire, F.; Collin, G. *J. Solid State Chem.* **1995**, *118*, 33.